

A Cross-direction Task Decoupling Network for Small Logo Detection

Sujuan Hou*, Xingzhuo Li*, Weiqing Min†, Jiacheng Li*, Jing Wang*, Yuanjie Zheng*, Shuqiang Jiang†
* School of Information Science and Engineering, Shandong Normal University
Jinan, China

† Key Laboratory of Intelligent Information Processing, Institute of Computing Technology, Chinese Academy of Sciences
Beijing, China

{hsj1985}@126.com, {2020317105, 2021317140}@stu.sdn.edu.cn,
{minweiqing, sqjiang}@ict.ac.cn, {jingwang1551}@163.com, {zhengyuanjie}@gmail.com

arXiv:2305.02503v1 [cs.CV] 4 May 2023

Abstract—Logo detection plays an integral role in many applications. However, handling small logos is still difficult since they occupy too few pixels in the image, which burdens the extraction of discriminative features. The aggregation of small logos also brings a great challenge to the classification and localization of logos. To solve these problems, we creatively propose Cross-direction Task Decoupling Network (CTDNet) for small logo detection. We first introduce Cross-direction Feature Pyramid (CFP) to realize cross-direction feature fusion by adopting horizontal transmission and vertical transmission. In addition, Multi-frequency Task Decoupling Head (MTDH) decouples the classification and localization tasks into two branches. A multi-frequency attention convolution branch is designed to achieve more accurate regression by combining discrete cosine transform and convolution creatively. Comprehensive experiments on four logo datasets demonstrate the effectiveness and efficiency of the proposed method.

Index Terms—object detection, logo detection, multi-scale feature, attention

I. INTRODUCTION

Logo detection is a special application of object detection in computer vision. It has drawn increasing attention for its various practical applications such as intelligent transportation, trademark infringement detection, and multimedia information collection and analysis.

With the increasing number of brands, the research of small logo detection algorithms still remains extremely challenging. (1) The first difficulty mainly lies in the small object regions, which has high requirements for feature extraction. Two car logos have similar backgrounds and logo shapes, and the small logo exacerbates the detection difficulties in Fig. 1 (a). It is difficult to extract distinguishing features from small logos since they have fewer features available and are more susceptible to external interference. (2) The second challenge is that the aggregation of small logos causes the difficulty of regression and classification. Due to practical needs such as merchandising and advertising shooting, the aggregation detection of logos is a widely occurring challenge in logo detection. An example of aggregation is shown in Fig. 1 (b).

This research was funded by the National Natural Science Foundation of China (62072289 and U19B2040), and CAAI-Huawei MindSpore Open Fund. Corresponding author: Weiqing Min.



(a) few available features



(b) the aggregation of small logos

Fig. 1. Small logo detection challenges: (a) small logos usually occupy too few pixels. (b) the aggregation of multiple small logos.

The two well-liked categories ‘Cocolino’ and ‘NIVEA’ are extensively concentrated. The bounding box of the aggregated region is too close to convergence and regression in logo detection.

The existing algorithms have been studied for small object detection, among which the feature fusion method has shown high performance [1]–[3]. In addition, many deep learning researchers have explored classification and localization [4]–[6]. However, there are three main problems that need to be solved when existing models are directly used to small logo detection. Firstly, the previous work mainly focused on the object detection of natural scene images, which often failed to achieve satisfactory results when it was directly applied to the small logo. Secondly, few existing studies have specifically analyzed the difficulty of small logo detection, while we analyzed it from two perspectives of few extractable features and logo aggregation. Finally, existing models are more suited to generic object detection, making it difficult to achieve a

proper trade-off between accuracy and speed when they are used in small logo detection.

In this paper, we propose a novel logo detection method Cross-direction Task Decoupling Network (CTDNet). It utilizes creative Cross-direction Feature Pyramid (CFP) to achieve more effective feature fusion in small logo regions. To solve the aggregation of small logos, the network decouples classification and localization tasks into two branches by introducing Multi-frequency Task Decoupling Head (MTDH). In CFP, we rethink the flow of feature information, adopting horizontal transmission and vertical transmission. An iterative feature pyramid is adopted for horizontal transmission, where the output features of the former pyramid are the good feature distribution of the latter pyramid. The vertical transmission after the horizontal transmission is focused on extracting balanced semantic representations, which enhances the feature information at each resolution. In MTDH, the fully-connected layer is utilized to build fully connected classification branch since it has a stronger ability to distinguish logo categories. To solve the aggregation difficulty of small logos, our proposed multi-frequency attention convolution branch complements the advantages of discrete cosine transform and convolution. Discrete cosine transform completes the focusing and extraction of important information in the image, while the feature transformation process of the convolutional layer determines its good sensitivity to position.

The main contributions of this paper can be summarized as follows:

- We propose Cross-direction Feature Pyramid (CFP) to build a simple and effective pyramid through horizontal transmission and vertical transmission.
- A multi-frequency attention convolution branch is designed to solve the logo aggregation difficulty by combining discrete cosine transform and convolution in Multi-frequency Task Decoupling Head (MTDH).
- We conduct extensive experiments on four benchmark logo datasets, including FlickrLogos-32, QMUL-OpenLogo, FoodLogoDet-1500, and LogoDet-3K. The experimental results demonstrate the effectiveness of the proposed model.

II. RELATED WORK

Object detection is one of the most basic problems in computer vision. In the era of deep learning, object detection is divided into two genres: two-stage and one-stage. The two-stage algorithm generates regional proposals based on the image content and then performs classification and bounding box localization [6]–[8]. The one-stage algorithm is characterized by generating the category and localization coordinates directly [9]–[11].

Logo detection has been extensively researched in many realistic applications. Early methods for logo detection generally relied on manual feature extraction techniques and traditional classification models. Recently, a series of deep logo detection methods as well as large-scale datasets have been proposed by

exploiting the state-of-the-art object detection models [12]–[15]. Logo-Yolo [13] was proposed to solve imbalanced samples of logos, and a high-quality logo dataset LogoDet-3K was built. MFDNet [14] was designed to address the multi-scale and similar logo difficulties in food logo detection, and a large dataset FoodLogoDet-1500 was constructed to solve data limitations. A cross-view learning method [12] provided ideas for logo detection. These methods promote the development of logo detection research, especially the detection problems in specific scenarios, such as the multi-scale and similarity of logo. Meanwhile, a series of high quality logo datasets have been established, which greatly facilitates future research work. However, few studies have focused on detection of small logos. Our work provides a solution and reference for small logo detection.

III. METHOD

In this section, we present a logo detection method CTDNet shown in Fig. 2. After extracting the basic features from the input image, the model first inputs the feature map into CFP to learn multi-scale features. Then the feature map is fed into Region Proposal Network (RPN) to obtain region proposals. Finally, the model is sent to MTDH for classification and localization. All components will be described in detail in the following sections.

A. Cross-direction Feature Pyramid

1) *Horizontal Transmission*: In this subsection, we first define the basic structure of FPN. S is the number of stages, e.g., $S = 4$. In Fig. 2, x_i is the connection of two pyramids. $m_i (\forall i = 1, \dots, S)$ denotes a set of output feature maps, and is defined as:

$$m_i = T_i(m_{i+1}, x_i), x_i = U_i(x_{i-1}) \quad (1)$$

where T_i represents the i -th top-down FPN operation and U_i indicates the i -th stage of the bottom-up backbone.

Our horizontal transmission adds feedback connections to FPN to form an iterative feature pyramid. As in Fig. 2, the output features of one pyramid are sent to the next one. The output feature m_i of iterative feature pyramid is defined as:

$$m_i = T_i(m_{i+1}, x_i), x_i = U_i(x_{i-1}, I_i(m_i)) \quad (2)$$

where I_i denotes the feature of the feedback connection to the backbone. Further, we expand the iterative feature pyramid as a sequential network. N is the number of expansions:

$$m_i^n = T_i^n(m_{i+1}^n, x_i^n), x_i^n = U_i^n(x_{i-1}^n, I_i^n(m_i^{n-1})) \quad (3)$$

2) *Vertical Transmission*: After the horizontal transmission, we extract the balanced semantic representation on the vertical transmission to strengthen the relationship between levels. In Fig. 2, we first resize all the feature maps to a medium size to obtain balanced features R :

$$R = \frac{1}{S} \sum_{r=r_{min}}^{r_{max}} R_r \quad (4)$$

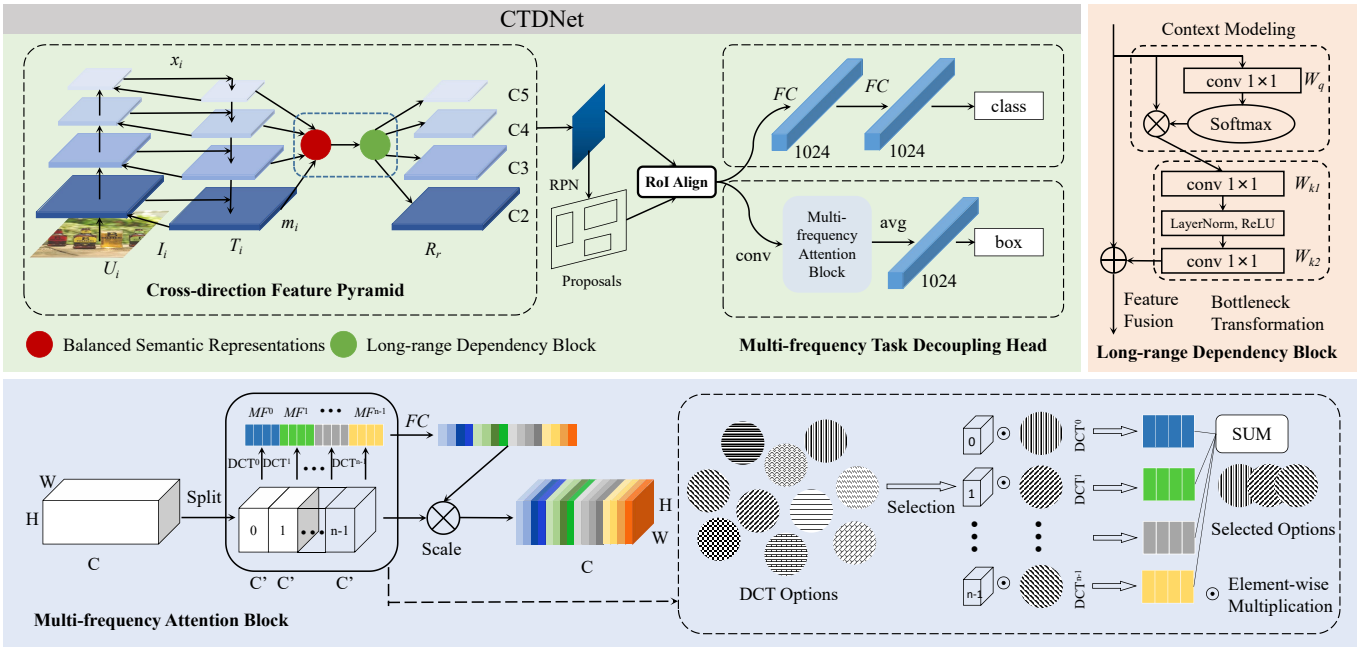


Fig. 2. Overview of proposed CTDNet for small logo detection. In multi-frequency attention block, DCT denotes Discrete Cosine Transform. For simplicity, DCT indices are represented in the one-dimensional format.

where S is the number of feature levels. The bottom and top resolution levels are labeled as r_{min} and r_{max} , respectively. R_r denotes the feature level with a resolution of r . Afterward, the obtained features are rescaled using the same but opposite way to complete the reinforcement.

To further optimize the extracted features, we capture the long-range dependency of the balanced features using global context modeling [16] in Fig. 2.

B. Multi-frequency Task Decoupling Head

After RoI Align, the localization and classification tasks are performed respectively by two different branches. In the localization branch, the feature transformation process is implemented using convolution to extract more discriminative features. Besides, the channel representation can be considered as a compression process using frequency analysis [17]. The channel informations are compactly encoded to maintain their representational capability. We use the discrete cosine transform to compress channels and take its multiple frequency components as the channel attention mechanism.

The multi-frequency attention block is shown in Fig. 2. We denote MF^i for a particular frequency component, which can be considered as channel attention pre-processing of the feature map X :

$$MF^i = \sum_{h=0}^{H-1} \sum_{w=0}^{W-1} X^i B_{h,w}^i \quad (5)$$

where i denotes the i -th group. (h, w) is the position of the 2D image. B is the basic function of the discrete cosine transform.

The complete vector MF can be obtained by the concatenation of multiple frequency components:

$$MF = \text{concat}([MF^0, MF^1, \dots, MF^{n-1}]) \quad (6)$$

The final multi-frequency attention block can be written as:

$$MFB = \text{sigmoid}(FC(MF)) \quad (7)$$

In the classification task, fully connected classification branch is adopted to strengthen the sensitivity of the logo category by combining two fully connected layers.

C. Loss Function

In the CTDNet, the final loss function consists of L_{rpn} , L_{fc} and L_{conv} :

$$L = L_{rpn} + \omega_{fc} L_{fc} + \omega_{conv} L_{conv} \quad (8)$$

where L_{rpn} , L_{fc} and L_{conv} are the losses for RPN, fully connected classification branch and multi-frequency attention convolution branch, respectively. ω_{fc} and ω_{conv} are the weights of the classification branch and the localization branch, respectively.

We realize L_{conv} by Smooth L1 Loss and L_{fc} by Cross-Entropy Loss function.

IV. EXPERIMENTS

A. Experimental Setting

To evaluate the effectiveness of the proposed CTDNet, we complete comprehensive experimental validation on four datasets. They include two small-scale datasets FlickrLogos-32 [18] and QMUL-OpenLogo [19], the medium-scale food

TABLE I
STATISTICS OF FOUR LOGO DATASETS.

Datasets	#Classes	#Images	#Objects	#Trainval	#Test	#Small Objects
FlickrLogos-32 [18]	32	2,240	3,405	1,478	762	185
QMUL-OpenLogo [19]	352	27,083	51,207	18,752	8,331	11,841
FoodLogoDet-1500 [14]	1,500	99,768	145,400	80,280	19,488	16,463
LogoDet-3K [13]	3,000	158,652	194,261	142,142	16,510	3,508

TABLE II
DETECTION RESULTS ON FOUR DATASETS (%).

Method	Backbone	FlickrLogos-32			QMUL-OpenLogo			FoodLogoDet-1500			LogoDet-3K						
		mAP	AP_S	AP_M	AP_L	mAP	AP_S	AP_M	AP_L	mAP	AP_S	AP_M	AP_L				
One-stage:																	
FSAF [4]	ResNet-50-FPN	84.9	26.5	78.9	89.9	48.7	31.0	50.4	60.0	83.4	69.4	71.8	78.5	63.0	26.4	56.0	67.1
ATSS [9]	ResNet-50-FPN	84.0	21.3	73.8	89.7	47.3	29.6	49.5	58.8	84.2	66.5	72.0	77.8	68.3	20.3	56.4	73.9
GFL [10]	ResNet-50-FPN	84.4	20.5	80.0	89.8	47.5	30.4	48.5	58.9	74.3	64.6	72.6	77.7	60.1	14.7	50.8	65.1
TOOD [20]	ResNet-50-FPN	87.7	19.3	84.5	93.9	51.9	33.3	52.7	63.6	82.7	74.0	79.9	86.5	78.5	40.0	73.3	81.9
DW [21]	ResNet-50-FPN	88.6	24.7	83.0	94.4	54.9	35.3	55.2	69.0	82.2	76.2	78.4	86.3	85.6	54.5	79.4	88.9
Two-stage:																	
Faster R-CNN [22]	ResNet-50-FPN	87.3	16.8	82.4	94.5	53.3	33.7	53.7	67.2	84.0	76.0	81.0	88.4	85.2	51.5	79.7	88.3
Cascade R-CNN [23]	ResNet-50-FPN	87.7	14.3	83.3	94.6	52.4	30.9	51.6	65.4	83.3	74.3	79.0	87.5	84.5	43.7	77.1	88.0
PANet [24]	ResNet-50-PAFPN	87.5	17.1	82.7	93.8	53.7	29.3	53.9	68.3	84.0	75.7	81.6	88.1	85.2	48.4	78.9	88.5
Libra R-CNN [3]	ResNet-50-BFP	88.6	22.1	87.0	94.2	56.5	35.1	57.5	69.3	83.3	76.5	80.6	87.2	82.6	52.2	77.7	85.8
Generalized IoU [25]	ResNet-50-FPN	86.5	18.9	82.1	93.6	52.4	31.3	52.9	65.5	83.5	74.3	80.6	87.7	84.2	48.4	78.9	87.4
Complete IoU [26]	ResNet-50-FPN	88.2	17.7	86.3	94.2	52.7	31.2	53.0	66.4	83.3	75.0	80.9	87.1	83.9	51.0	78.6	86.9
Dynamic R-CNN [7]	ResNet-50-FPN	87.6	23.2	82.7	94.5	53.1	30.9	53.5	66.5	84.4	75.7	81.2	88.6	87.7	56.2	82.1	90.6
Double-head R-CNN [6]	ResNet-50-FPN	88.2	23.1	86.4	94.3	54.2	32.9	54.3	67.3	85.5	78.3	82.2	89.6	86.4	48.3	79.8	89.8
SABL [5]	ResNet-50-FPN	87.6	10.1	86.9	94.9	54.8	33.1	55.3	68.8	83.3	72.4	79.4	88.2	85.1	42.2	78.7	88.7
Sparse R-CNN [8]	ResNet-50-FPN	80.1	20.2	71.0	87.5	52.2	35.3	53.9	63.9	81.8	77.5	79.9	85.7	37.9	40.3	46.4	40.7
Guided Anchoring [27]	ResNet-50-FPN	86.8	11.7	82.5	93.5	52.2	32.7	53.7	65.9	85.4	77.2	82.6	89.0	86.3	56.5	81.6	89.4
CTDNet(ours)	ResNet-50-CFP	89.7	34.3	89.0	94.3	58.4	37.6	60.7	71.7	85.6	79.8	83.1	88.8	88.2	58.4	82.9	90.8

TABLE III
EVALUATING INDIVIDUAL COMPONENT ON FOUR DATASETS (%).

Method	Backbone	FlickrLogos-32			QMUL-OpenLogo			FoodLogoDet-1500			LogoDet-3K						
		mAP	AP_S	AP_M	AP_L	mAP	AP_S	AP_M	AP_L	mAP	AP_S	AP_M	AP_L				
Faster R-CNN	ResNet-50-FPN	87.3	16.8	82.4	94.5	53.3	33.7	53.7	67.2	84.0	76.0	81.0	88.4	85.2	51.5	79.7	88.3
Faster R-CNN+CFP	ResNet-50-CFP	88.5	24.2	87.6	94.6	57.3	36.1	58.5	70.1								
Faster R-CNN+MTDH	ResNet-50-FPN	88.6	21.6	86.5	94.7	55.5	34.8	56.2	67.6								
Faster R-CNN+CFP+MTDH	ResNet-50-CFP	89.7	34.3	89.0	94.3	58.4	37.6	60.7	71.7								
Faster R-CNN	ResNet-50-FPN	84.0	76.0	81.0	88.4	85.2	51.5	79.7	88.3								
Faster R-CNN+CFP	ResNet-50-CFP	85.5	77.1	82.5	89.6	85.9	55.9	81.1	88.9								
Faster R-CNN+MTDH	ResNet-50-FPN	85.1	77.6	82.1	88.9	87.2	58.5	81.8	90.1								
Faster R-CNN+CFP+MTDH	ResNet-50-CFP	85.6	79.8	83.1	88.8	88.2	58.4	82.9	90.8								

TABLE IV
LOGO METHOD DETECTION RESULTS ON TWO DATASETS (%).

Method	Backbone	FlickrLogos-32	QMUL-OpenLogo
Logo-Yolo [13]	DarkNet-53	76.1	53.2
OSF-Logo [28]	ResNet-50-FPN	87.0	53.3
MFDNet [14]	ResNet-50-BFP	86.2	51.3
DSFP-GA [29]	ResNet-50-DSFP	87.1	54.0
CTDNet(ours)	ResNet-50-CFP	89.7	58.4

TABLE V
EXPERIMENTS ON PARAMETER SENSITIVITY.

Method	Group Number	Loss Weight	mAP(%)
Faster R-CNN(baseline)	-	-	87.3
Faster R-CNN+MTDH	c4f2	0.5	87.9
Faster R-CNN+MTDH	c4f2	1.0	87.8
Faster R-CNN+MTDH	c4f2	2.0	88.6
Faster R-CNN+MTDH	c6f4	2.0	88.4
CTDNet(ours)	c4f2	0.5	86.7
CTDNet(ours)	c4f2	1.0	88.6
CTDNet(ours)	c4f2	2.0	89.7
CTDNet(ours)	c6f4	2.0	89.2

dataset FoodLogoDet-1500 [14], and the large-scale dataset LogoDet-3K [13]. The detailed description of these datasets is shown in Table I.

We implement our method based on the publicly available MMDetection toolbox [30]. For evaluation, we use the widely used mean Average Precision (mAP) [31], with an IoU threshold of 0.5. Considering different sizes of logos, we adopt AP_S , AP_M , AP_L respectively, where AP_S is the Average Precision (AP) for small logo objects (area $< 32^2$), AP_M is the AP for medium logo objects ($32^2 < \text{area} < 96^2$), and AP_L is the AP for large logo objects (area $> 96^2$). In our experiments, the basic detection network is trained using Stochastic Gradient Descent (SGD), and the initial learning rate is set to 0.002. The input images are resized to 1000×600 , the weight decay is 0.0001, and the momentum is 0.9. We follow the settings in MMDetection for other hyperparameters.

B. Main Results

In this subsection, we show the main results of CTDNet conducted on four datasets. To validate the generality of the

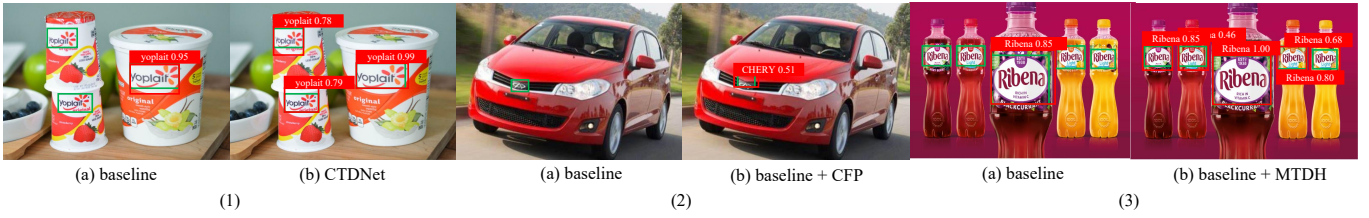


Fig. 3. Comparison of visualization results between baseline and CTDNet. Green box: ground-truth box. Red box: the location of the detected logo.

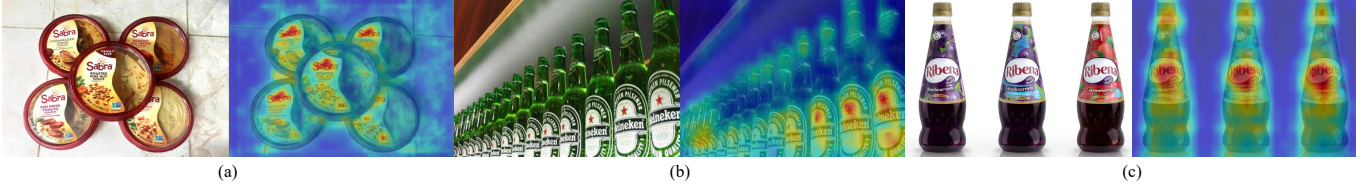


Fig. 4. Heatmap visualization by cross-direction feature pyramid.

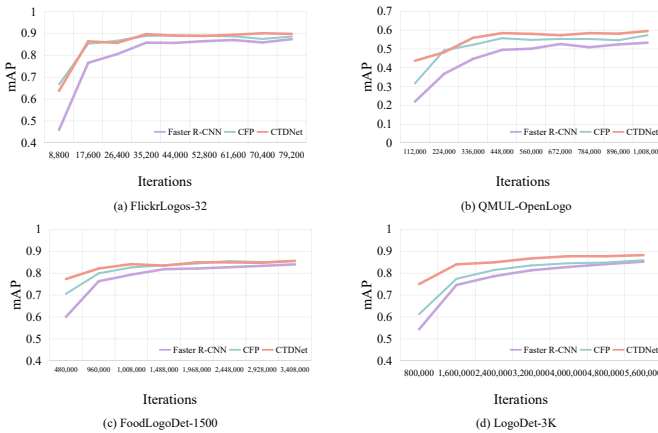


Fig. 5. Comparison between different strategies with increasing number of iterations.

proposed CTDNet, we compare the proposed model with several other popular baselines, including one-stage series and two-stage series, as reported in Table II. For a fair comparison with other detectors, we equip all baselines with ResNet-50 and FPN as the backbone. On all four datasets, we observe that the proposed CTDNet method is superior to other baselines, which achieves the best performance with mAP and AP_S . The proposed CTDNet strategy produces dominant performance compared to other approaches utilizing feature fusion, like PANet and Libra R-CNN. To examine the effectiveness for detection head, we use Double-head R-CNN and SABL as comparison methods. Under evaluation metrics of mAP and AP_S , we can see that CTDNet obtains better performance than them.

In Table IV, more contrastive experiments with logo-detection-oriented methods are conducted on FlickrLogos-32 and QMUL-OpenLogo, including Logo-Yolo [13], OSF-Logo [28], MFDNet [14] and DSFP-GA [29].

C. Ablation Studies

In this subsection, we show the ablation studies of CFP and MTDH on four datasets in Table III. The mAP, AP_S , AP_M and AP_L for accuracy are applied to the reported results. We use Faster R-CNN equipped with ResNet-50 and FPN as the baseline.

1) *Quantitative Analysis*: From Table III, we can see that both the CFP and MTDH gain improvement on four datasets. On LogoDet-3K, CFP gets 0.7% mAP more than Faster R-CNN, while MTDH improves 2.0% mAP. The combination of CFP and MTDH brings the best performance to the model. In addition, CTDNet gains 2.4%, 5.1%, and 1.6% mAP improvement in comparison with baseline on FlickrLogos-32, QMUL-OpenLogo, and FoodLogoDet-1500, respectively. Both CFP and MTDH can improve AP_S on four datasets, which illustrates the improvement of small logo detection performance by these two components. In comparison with the baseline, our model improves the AP_S by 17.5%, 3.9%, 3.8% and 6.9% on FlickrLogos-32, QMUL-OpenLogo, FoodLogoDet-1500, and LogoDet-3K, respectively. The ablation study shows that the formulations of CFP and MTDH have the best configuration.

2) *Visualization Analysis*: Fig. 3 provides the visualization results by Faster-RCNN (hereinafter referred to as baseline), ‘baseline + CFP’, ‘baseline + MTDH’ and CTDNet from the localization and accuracy of testing on LogoDet-3K. As seen in Fig. 3 (1), CTDNet is far superior to baseline in both localization and accuracy. It is worth mentioning that logo categories ‘yoplait’ and ‘CHERY’ can not be detected by baseline, while our model obtains good detection results in Fig. 3 (1) (2). These results demonstrate that CFP is consistent with our intuition concerning a non-negligible improvement in feature fusion. From the comparison between baseline and ‘baseline + MTDH’, as shown in Fig. 3 (3), baseline only detects the largest logo in the category ‘Ribena’, while ‘baseline + MTDH’ detects all five logos. These results indicate that our detection head plays a very critical role in detecting the

aggregation of small logos.

Fig. 4 gives two illustrative examples of the heatmap visualization results by CFP. The bright colors in the figure represent that CFP extracts more representative feature information at this location. Comparing with the original image, it can be seen that the concerned positions of CFP are well aligned with detection logos. These results further prove the effectiveness of our designed CFP.

3) *Parameter Sensitivity*: Different iteration times are set to compare baseline, CFP and CTDNet in terms of convergence and accuracy. As can be seen from Fig. 5 that with the increase of iteration times, the three models all achieve performance convergence on the four data sets, among which CTDNet achieves the best performance.

For MTDH, the comparative experiments on group numbers and loss weights are conducted. Table V shows the performance of baseline, MTDH and CTDNet with different parameter settings on FlickrLogos-32. For the loss weights, we set three values of 0.5, 1.0 and 2.0. For the number of groups, we set two types, namely c6f4 and c4f2. The former represents 6 convolutional layers and 4 fully connected layers, while the latter represents 4 convolutional layers and 2 fully connected layers. According to Table V, it can be seen that all three values of loss weights enable MTDH and CTDNet to obtain performance improvements compared to the baseline. Both MTDH and CTDNet obtain the best performance when the loss weight is 2.0 and the group number is c4f2.

V. CONCLUSION

In this paper, we propose a logo detection model Cross-direction Task Decoupling Network (CTDNet), which introduces CFP and MTDH to address the detection difficulties caused by small logos. The proposed CFP utilizes a simple pyramid to accomplish feature fusion through horizontal transmission and vertical transmission. Meanwhile, MTDH is proposed to build different head structures for classification and localization tasks, which can solve the logo aggregation difficulty by combining discrete cosine transform and convolution. In future, we will focus on other challenges of logo detection, such as low resolution, logos with large aspect ratios and similar logos.

REFERENCES

- [1] T.-Y. Lin, P. Dollár, R. Girshick, K. He, B. Hariharan, and S. Belongie, "Feature pyramid networks for object detection," in *CVPR*, 2017, pp. 2117–2125.
- [2] S. Qiao, L.-C. Chen, and A. Yuille, "Detectors: Detecting objects with recursive feature pyramid and switchable atrous convolution," in *CVPR*, 2021, pp. 10 213–10 224.
- [3] J. Pang, K. Chen, J. Shi, H. Feng, W. Ouyang, and D. Lin, "Libra r-cnn: Towards balanced learning for object detection," in *CVPR*, 2019, pp. 821–830.
- [4] C. Zhu, Y. He, and M. Savvides, "Feature selective anchor-free module for single-shot object detection," in *CVPR*, 2019, pp. 840–849.
- [5] J. Wang, W. Zhang, Y. Cao, K. Chen, J. Pang, T. Gong, J. Shi, C. C. Loy, and D. Lin, "Side-aware boundary localization for more precise object detection," in *ECCV*, 2020, pp. 403–419.
- [6] Y. Wu, Y. Chen, L. Yuan, Z. Liu, L. Wang, H. Li, and Y. Fu, "Rethinking classification and localization for object detection," in *CVPR*, 2020, pp. 10 186–10 195.
- [7] H. Zhang, H. Chang, B. Ma, N. Wang, and X. Chen, "Dynamic r-cnn: Towards high quality object detection via dynamic training," in *ECCV*, 2020, pp. 260–275.
- [8] P. Sun, R. Zhang, Y. Jiang, T. Kong, C. Xu, W. Zhan, M. Tomizuka, L. Li, Z. Yuan, C. Wang *et al.*, "Sparse r-cnn: End-to-end object detection with learnable proposals," in *CVPR*, 2021, pp. 14 454–14 463.
- [9] S. Zhang, C. Chi, Y. Yao, Z. Lei, and S. Z. Li, "Bridging the gap between anchor-based and anchor-free detection via adaptive training sample selection," in *CVPR*, 2020, pp. 9759–9768.
- [10] X. Li, W. Wang, L. Wu, S. Chen, X. Hu, J. Li, J. Tang, and J. Yang, "Generalized focal loss: Learning qualified and distributed bounding boxes for dense object detection," *NeurIPS*, vol. 33, pp. 21 002–21 012, 2020.
- [11] Z. Ge, S. Liu, F. Wang, Z. Li, and J. Sun, "Yolox: Exceeding yolo series in 2021," *arXiv preprint arXiv:2107.08430*, 2021.
- [12] J. Wang, Y. Zheng, J. Song, and S. Hou, "Cross-view representation learning for multi-view logo classification with information bottleneck," in *ACM Multimedia*, 2021, pp. 4680–4688.
- [13] J. Wang, W. Min, S. Hou, S. Ma, Y. Zheng, and S. Jiang, "Logodet-3k: A large-scale image dataset for logo detection," *TOMM*, vol. 18, no. 1, pp. 1–19, 2022.
- [14] Q. Hou, W. Min, J. Wang, S. Hou, Y. Zheng, and S. Jiang, "Foodlogodet-1500: A dataset for large-scale food logo detection via multi-scale feature decoupling network," in *ACM Multimedia*, 2021, pp. 4670–4679.
- [15] S. Hou, J. Li, W. Min, Q. Hou, Y. Zhao, Y. Zheng, and S. Jiang, "Deep learning for logo detection: A survey," *arXiv preprint arXiv:2210.04399*, 2022.
- [16] Y. Cao, J. Xu, S. Lin, F. Wei, and H. Hu, "Gcnet: Non-local networks meet squeeze-excitation networks and beyond," in *ICCV*, 2019, pp. 0–0.
- [17] Z. Qin, P. Zhang, F. Wu, and X. Li, "Fcanet: Frequency channel attention networks," in *ICCV*, 2021, pp. 783–792.
- [18] S. Romberg, L. G. Pueyo, R. Lienhart, and R. Van Zwol, "Scalable logo recognition in real-world images," in *MIR*, 2011, pp. 1–8.
- [19] H. Su, X. Zhu, and S. Gong, "Open logo detection challenge," *arXiv preprint arXiv:1807.01964*, 2018.
- [20] C. Feng, Y. Zhong, Y. Gao, M. R. Scott, and W. Huang, "Tood: Task-aligned one-stage object detection," in *ICCV*. IEEE Computer Society, 2021, pp. 3490–3499.
- [21] S. Li, C. He, R. Li, and L. Zhang, "A dual weighting label assignment scheme for object detection," in *CVPR*, 2022, pp. 9387–9396.
- [22] S. Ren, K. He, R. Girshick, and J. Sun, "Faster r-cnn: Towards real-time object detection with region proposal networks," *NeurIPS*, vol. 28, 2015.
- [23] Z. Cai and N. Vasconcelos, "Cascade r-cnn: Delving into high quality object detection," in *CVPR*, 2018, pp. 6154–6162.
- [24] S. Liu, L. Qi, H. Qin, J. Shi, and J. Jia, "Path aggregation network for instance segmentation," in *CVPR*, 2018, pp. 8759–8768.
- [25] H. Rezatofighi, N. Tsoi, J. Gwak, A. Sadeghian, I. Reid, and S. Savarese, "Generalized intersection over union: A metric and a loss for bounding box regression," in *CVPR*, 2019, pp. 658–666.
- [26] Z. Zheng, P. Wang, W. Liu, J. Li, R. Ye, and D. Ren, "Distance-iou loss: Faster and better learning for bounding box regression," in *AAAI*, vol. 34, no. 07, 2020, pp. 12 993–13 000.
- [27] J. Wang, K. Chen, S. Yang, C. C. Loy, and D. Lin, "Region proposal by guided anchoring," in *CVPR*, 2019, pp. 2965–2974.
- [28] Y. Meng, S. Hou, J. Wang, W. Jia, Y. Zheng, and A. Karim, "An adaptive representation algorithm for multi-scale logo detection," *Displays*, vol. 70, p. 102090, 2021.
- [29] B. Zhang, S. Hou, A. Karim, J. Wang, W. Jia, and Y. Zheng, "Discriminative semantic feature pyramid network with guided anchoring for logo detection," *Mathematics*, vol. 11, no. 2, p. 481, 2023.
- [30] K. Chen, J. Wang, J. Pang, Y. Cao, Y. Xiong, X. Li, S. Sun, W. Feng, Z. Liu, J. Xu *et al.*, "Mmdetection: Open mmlab detection toolbox and benchmark," *arXiv preprint arXiv:1906.07155*, 2019.
- [31] M. Everingham, L. Van Gool, C. K. Williams, J. Winn, and A. Zisserman, "The pascal visual object classes (voc) challenge," *IJCV*, vol. 88, no. 2, pp. 303–338, 2010.